Marine Geology 280 (2011) 130–142

Contents lists available at ScienceDirect

Marine Geology

journal homepage: www.elsevier.com/locate/margeo

# Distribution and provenance of wind-blown SE Pacific surface sediments

Cornelia Saukel [a,*], Frank Lamy [a], Jan-Berend W. Stuut [b,c], Ralf Tiedemann [a], Christoph Vogt [d]

[a] Alfred-Wegener-Institute for Polar and Marine Research (AWI), Postfach 12 01 61, 27568 Bremerhaven, Germany
[b] Marum, Center for Marine Environmental Sciences, Leobener Straße, 28359 Bremen, Germany
[c] NIOZ-Royal Netherlands Institute for Sea Research, P.O. Box 59, 1790 AB Den Burg, The Netherlands
[d] University of Bremen, Crystallography/ZEKAM, FB05 Geowissenschaften/Geo Sciences, P.O. Box 330440, 28334 Bremen, Germany

ARTICLE INFO

*Article history:*
Received 24 May 2010
Received in revised form 11 November 2010
Accepted 11 December 2010
Available online 17 December 2010

Communicated by G.J. de Lange

*Keywords:*
SE Pacific
clay-mineral assemblages
eolian dust
grain-size distribution
trade winds

ABSTRACT

The reconstruction of low-latitude ocean–atmosphere interactions is one of the major issues of (paleo-) environmental studies. The trade winds, extending over 20° to 30° of latitude in both hemispheres, between the subtropical highs and the intertropical convergence zone, are major components of the atmospheric circulation and little is known about their long-term variability on geological time-scales, in particular in the Pacific sector. We present the modern spatial pattern of eolian-derived marine sediments in the eastern equatorial and subtropical Pacific (10°N to 25°S) as a reference data set for the interpretation of SE Pacific paleo-dust records. The terrigenous silt and clay fractions of 75 surface sediment samples have been investigated for their grain-size distribution and clay-mineral compositions, respectively, to identify their provenances and transport agents.

Dust delivered to the southeast Pacific from the semi- to hyper-arid areas of Peru and Chile is rather fine-grained (4–8 μm) due to low-level transport within the southeast trade winds. Nevertheless, wind is the dominant transport agent and eolian material is the dominant terrigenous component west of the Peru–Chile Trench south of ~5°S. Grain-size distributions alone are insufficient to identify the eolian signal in marine sediments due to authigenic particle formation on the sub-oceanic ridges and abundant volcanic glass around the Galapagos Islands. Together with the clay-mineral compositions of the clay fraction, we have identified the dust lobe extending from the coasts of Peru and Chile onto Galapagos Rise as well as across the equator into the doldrums. Illite is a very useful parameter to identify source areas of dust in this smectite-dominated study area.



## 1. Introduction

The Peruvian and Chilean coasts as well as the Altiplano of Peru, Bolivia and Chile belong to the most arid areas worldwide and are recognized emission sources of eolian dust (e.g., Goudie and Middleton, 2006; Jickells et al., 2005; Joussaume, 1990; Li et al., 2008; Prospero et al., 2002). This region has experienced much less attention within the dust-studying community (e.g., Maher et al., 2010; Pye, 1987; Tegen et al., 2002; Werner et al., 2002), as dust transport to the tropical east and subtropical southeast Pacific is considerably smaller than, e.g., that off west Africa, in the Arabian Sea, off east China or Australia. However, basins such as the Salar de Uyuni on the Bolivian Altiplano are comparable in size to the Bodélé depression in Chad, one of the major dust sources in Africa, or to Lake Eyre in Australia (Goudie and Middleton, 2006). Nevertheless, dust sources in the Southern Hemisphere are generally smaller than those of the Northern Hemisphere (Maher et al., 2010). The tropical east Pacific, however, is a key location for (paleo-)climate research, as atmosphere-ocean linkages such as the El Niño/Southern Oscillation system or past shifts of the intertropical convergence zone (ITCZ) on glacial–interglacial time scales are still controversial (e.g., Leduc et al., 2009; Rincón Martínez et al., 2010). Therefore, the role of eolian dust may be larger than hitherto acknowledged, and forms a vital gap in our knowledge and understanding of the region.

Atmospheric dust particles represent a link between the atmosphere, lithosphere and the hydrosphere (Arimoto, 2001; Maher et al., 2010; Ridgwell, 2002) and are thus a valuable parameter in the pursuit of understanding the climate system. The concentration of mineral aerosols (dust) is a relevant feature within the global climate system. Its variability may cause changes in, e.g., the radiative forcing through absorption and scattering of light, in the provision of nutrients to marine ecological systems or in cloud cover through the availability of more or less condensation nuclei (Harrison et al., 2001). Furthermore, dust and its grain-size distribution can be used to study changes in continental aridity/humidity, spatial variations of major wind patterns as well as changes in wind intensity (Arimoto, 2001; Rea, 1994; Sarnthein et al., 1981; Stuut et al., 2002). Hence, proxy-

* Corresponding author. Tel.: +49 471 4831 2120; fax: +49 471 4831 1923.
*E-mail addresses:* Cornelia.Saukel@awi.de (C. Saukel), Frank.Lamy@awi.de (F. Lamy), Jan-Berend.Stuut@nioz.nl (J.-B.W. Stuut), Ralf.Tiedemann@awi.de (R. Tiedemann), cvogt@uni-bremen.de (C. Vogt).

0025-3227/$ – see front matter © 2010 Elsevier B.V. All rights reserved.
doi:10.1016/j.margeo.2010.12.006

based reconstruction of atmospheric changes in the (sub-)tropical east Pacific provide important clues for understanding past changes in ocean–atmosphere dynamics related to e.g. the Southern Oscillation, the trade winds and associated ITCZ shifts.

In order to tackle the importance of recent wind-transported material in the eastern equatorial Pacific and its sources, Prospero and Bonatti (1969) sampled atmospheric dust during a cruise of RV Pillsbury in 1967. They concluded that the supply of eolian dust to ocean sediments south of the ITCZ is less than on its northern side, and identified the arid coastal areas of Peru and northern Chile (Atacama Desert) as the source for those samples collected south of the ITCZ . Several subsequent studies, however, stressed eolian dust to be a noteworthy contributor to (south-)eastern Pacific deep-sea sediments (e.g., Dauphin, 1983; Heath et al., 1974; Krissek et al., 1980; Molina-Cruz and Price, 1977; Prospero et al., 2002; Rea, 1994; Rosato et al., 1975; Scheidegger and Krissek, 1982). Molina-Cruz and Price (1977) described the quartz distribution in surface sediments extending in a tongue similar in direction and position as the prevailing trade winds and interpreted the quartz-rich sediments to be of eolian origin. Rosato and Kulm (1981) investigated the clay-mineral assemblages of surface sediments on the continental margin and Nazca Plate. Krissek et al. (1980) could not distinguish different agents of transport for terrigenous input with the help of grain-size and element analyses in the area but found bottom nepheloid layers in the Peru Basin. Scheidegger and Krissek (1982) concentrated on quartz and feldspar contents in different grain-size classes inferring dispersal patterns and deposition of eolian and fluvial sediments off Peru and northern Chile. According to their interpretations, eolian-derived material dominates sediments west of the Peru–Chile Trench. Dauphin (1983) used the size of quartz grains as an indicator of provenance and paleo-winds. Besides the South American arid areas, he identified another dust source north of the equator for sediments around the East Pacific Rise. Boven and Rea (1998) attempted to separate the eolian and hemipelagic components in a sediment core 300 km west of the mouth of the Gulf of Guayaquil. Even though the core is largely influenced by hemipelagic sedimentation (Boven and Rea, 1998) due to enormous river discharges through the gulf (Rincón Martínez et al., 2010), they identified the eolian component as the dominant contributor of terrigenous material after 15 ka.

The focus of our study is to retrieve the modern spatial pattern of mineral dust as preserved in deep-sea sediments of the SE Pacific, in order to investigate the relation of the southeast trade winds and their dust transport. Our approach differs from former studies in that we used two independent parameters: We measured grain-size distributions of the siliciclastic silt fraction (2–63 μm) with a laser particle sizer and the clay-mineral composition of the clay fraction (<2 μm) with X-ray diffraction (XRD) to identify the eolian signal in sea surface sediments. Subsequently, we applied an end-member analysis (Weltje, 1997) to the grain-size data and a cluster analysis to the clay-mineral composition data. This enabled us to relate different grain-size populations (end-members) to distinct sources and means of transport. The end-member modeling algorithm (EMMA) has been successfully applied on Atlantic surface sediment samples offshore West Africa before (Holz et al., 2004; Weltje and Prins, 2003). We used it to interpret a set of surface sediment samples from the SE Pacific for the first time.

The tropical and subtropical east Pacific comprises upwelling regions as well as sub-aqueous volcanism and areas of strong bottom-water currents, among other features. It thus has a very complex sedimentary environment experiencing coeval and subsequent sedimentation and redistribution processes (Krissek et al., 1980; Scheidegger and Krissek, 1982), especially by bottom-water currents in the Panama Basin (Honjo, 1982; Kienast et al., 2007; Lonsdale, 1977; Lyle et al., 2007). This complicates the detection of the lithogenic eolian fraction and its distinction from fluvial input and sub-aqueous volcanic debris.

## 2. Physical setting

Our study area extends from 10°N–25°S and 70°–100°W (Fig. 1). It stretches from the equatorial doldrums in the north to the tropic–subtropical transition in northern Chile, covering the entire length of the Southern Hemisphere tropics in the east Pacific, plus the inner tropics of the Northern Hemisphere. Surface ocean circulation in the eastern tropical and subtropical Pacific is strongly influenced by wind forcing (Kessler, 2006), which, in turn, is determined by the topography of the Andes (Figs. 1 and 2). The continental topography and the Humboldt Current (Fig. 1) both largely influence the region's climatic conditions.

### 2.1. The climate of Central and (north-)western South America

Besides orographic effects, latitudinal shifting atmospheric pressure belts and prevailing winds determine precipitation and its distribution in Central and northern South America. The climate is generally seasonal, with distinct (boreal) winter dry periods, dominated by the subtropical high pressure, and wet summers, controlled by the equatorial low pressure (Bundschuh et al., 2007). Between 10°N and 10°S rains follow the overhead passage of the sun, and the equator experiences two wet and dry seasons (Schwerdtfeger, 1976). Colombia experiences rainfall of several m/yr (Potter, 1994; Schwerdtfeger, 1976).

In Ecuador, the area north of 3°S is also very humid. The elongated coastal desert, however, begins at ~1°S with cool Pacific waters offshore and a precipitation of 172 mm/a (Schwerdtfeger, 1976). At the immediate coast, sand and dust are omnipresent, while the northern banks of the Gulf of Guayaquil and the northern coastline of Ecuador are covered by tropical rain forest (Schwerdtfeger, 1976).

South of 3°S, a wet and dry seasonal regime with the rainy season lasting from November through April is prevalent, as typical for the Southern Hemispheric (sub-)tropics. Northern Peru is similar in relief and precipitation patterns to Ecuador. Central and South Peru are no longer affected by the ITCZ and the Western Cordillera forms a barrier for the atmospheric circulation south of 8°S. The Peruvian highlands experience moderate rainfall and the western slopes represent a transitional zone between the wet eastern regions and the extremely dry coastal plain. The central Peruvian coastal plain receives some precipitation in the form of drizzle through dense stratocumulus clouds, which are always present between May and October and frequent in April and November (Schwerdtfeger, 1976). During the normally dry summers, the sparse vegetation disappears from November on, and the landscape transforms back into a desert, which is a characteristic for the lower western slopes of the Andes (Schwerdtfeger, 1976). North of 12°S, however, heavy sierra rains occasionally spill over the Andes reaching the coastal plain. The regular switch of humid and dry conditions in this semi-arid part of Peru is a prerequisite for dust production as water-involved weathering processes are much more efficient in producing aerosols than eolian processes (Maher et al., 2010; Pye, 1987).

Generally, the south is drier than the north, so that the dust and rock plateau around Arequipa is mostly without vegetation. This plateau and the coastal desert, stretching south along the entire coastline to 27°S, belong to an extensive arid zone that extends from southernmost Ecuador across the Andes in southern Peru, Bolivia and northern Chile to southern Argentina (Schwerdtfeger, 1976) into the so-called “Arid Diagonale” (Bruniard, 1982). As a consequence, rainfall in the Atacama Desert, one of the driest areas on earth, reaches only a few mm/yr (Potter, 1994; Schwerdtfeger, 1976).

### 2.2. The wind regime in western South America and the SE Pacific

The southeastern Pacific subtropical anticyclone (SPSA) largely determines the atmospheric circulation in the study area. It influences

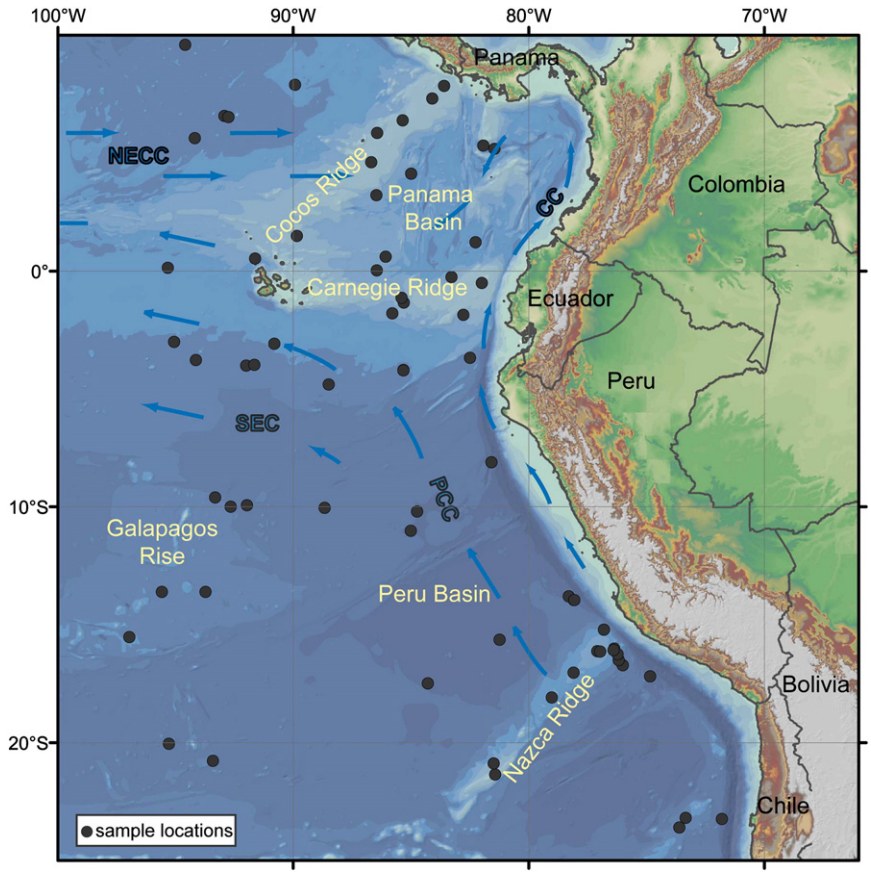


**Fig. 1.** Working area. Black dots show surface sample locations, blue arrows represent surface water currents. NECC — North Equatorial Counter Current; SEC — South Equatorial Current; PCC — Peru–Chile Current (Humboldt Current); and CC — Coastal Current.

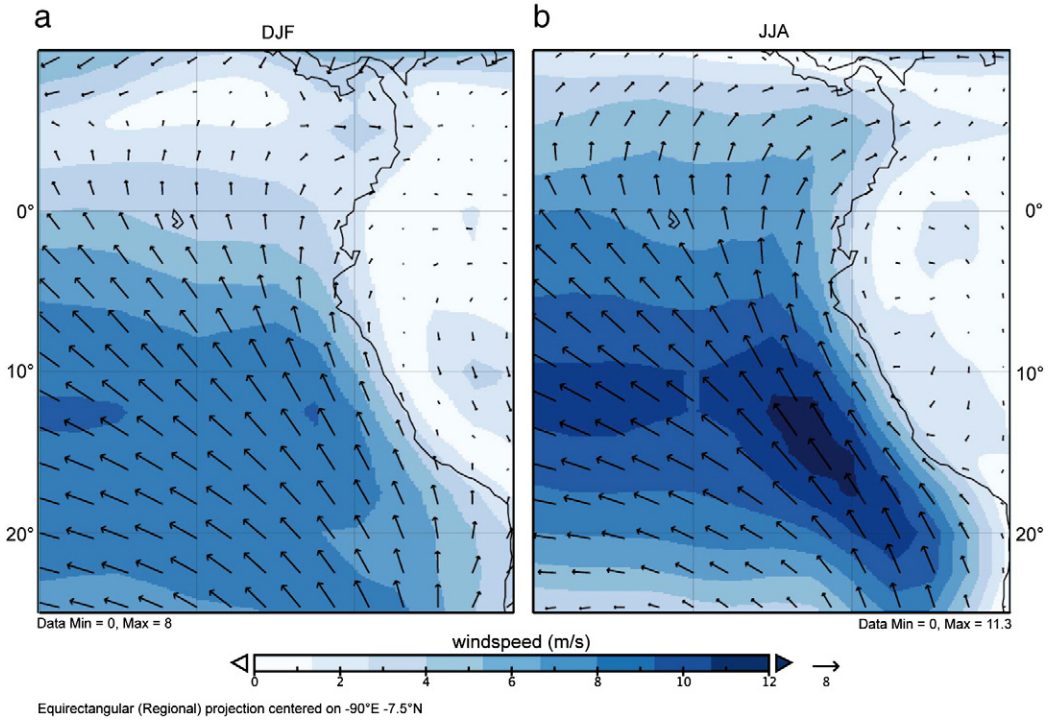


**Fig. 2.** Climatological winds during austral summer and winter in the (sub-)tropical east Pacific. Winds are averaged from the NCEP reanalysis (Kalnay et al., 1996). (a) Average wind speed during summer (December–February) and (b) winter (June–August).

the (sub-)tropical west coast of South America year-round. This results in predominant southerly low-level winds, which turn into the southeast trade winds further offshore (Garreaud and Muñoz, 2005). The Pacific trade winds represent one of the largest and most consistent wind fields on earth. They are strongest during their respective winter and spring months (Wyrtki and Meyers, 1976) (Fig. 2).

The SPSA is confined by the Intertropical Convergence Zone (ITCZ) and the polar front, to the north and south respectively. The ITCZ, coinciding with the northern boundary of the study area, shifts from roughly 13°N in austral winter (June–September) to 5°N in austral summer (December–March) (Kalnay et al., 1996; Strub et al., 1998) (Fig. 2). Together with the land–sea thermal contrasts, it influences surface winds as far as 5°S (Strub et al., 1998).

The eastern flank of the low-level anticyclonic circulation with south to southeasterly directions is very consistent in speed and direction above southern and alongshore Peru and northern Chile throughout the year. It is responsible for the distribution of dust over the ocean. According to Garreaud and Muñoz (2005), Howard (1985), and Lettau and Costa (1978), the coastal southerlies represent a low-level jet that is oriented along the coast within the maritime layer. It is characterized by a maximum of ~10 $ms^{-1}$ surface wind speed about 150 km offshore (Garreaud and Muñoz, 2005) (Fig. 2). This flow induces near-shore upwelling of cold water, which, in turn, is important for the thermal balance of the jet and strongly contributes to the aridity on land. At heights of 3–4 km, winds result from subsiding foehn circulation over the Andes from the Amazon basin and are thus easterly in direction (Howard, 1985; Rutllant et al., 2003). There are two circulation cells, above and beneath the subsidence inversion base, the upper of which is the more energetic. Its circulation is caused by the thermal contrast between the top of the marine boundary layer and the heated arid western slope of the Andes (Rutllant et al., 2003 Fig. 9). Dust from Peru and Chile is incorporated in the lower atmosphere by local relief and southern winds, which often have an onshore and upslope component (e.g., Flores-Aqueveque et al., 2010; Garreaud et al., 2003; Howard, 1985; Schwerdtfeger, 1976). Wind erosion is associated with wind gusts (Flores-Aqueveque et al., 2010; Kurgansky et al., 2010). Supposedly, the dust is thus lifted into higher air layers and carried by the SE trade winds, which distribute it above the ocean.

Wind speeds at the southern coasts of Peru vary between 4 and 8 kn (2–4 m/s), becoming stronger further north, reaching an average of 13 kn (6.7 m/s) at 9°S and up to 10 kn (5.1 m/s) elsewhere along the coast (Schwerdtfeger, 1976) (Fig. 2).

### 2.3. Andean geology

The clay mineral composition of terrigenous sediments as investigated in this study is – among other factors such as weathering conditions – dependent on its source-rocks on land (Chamley, 1989). The Andes are a magmatic mountain range with omnipresent metamorphic rocks. Their surface is mostly formed by volcanoes and granitic peaks. The absence of stratovolcanoes between 2°S and 15°S, representing a change in rock composition, is of particular interest. This volcanic gap in north–central Peru is caused by a flat subduction angle of the oceanic plate (Nur and Ben-Avraham, 1981). While the volcanic cover of the northern Andes is composed of more basic andesites and quartzandesites, ignimbrites consisting of andesites as well as alkaline rhyolites to rhyodacites cover the Central Andes (Zeil, 1986). Precambrian shields outcrop in places in southern Peru and Chile.

Central Andean soils are mostly immature due to the combination of aridity, low temperatures, intense erosion, and frequent ash falls in and adjacent to the volcanic zones. The Pacific lowlands bordering the mountain range often display thick alluvial deposits (Potter, 1994).

### 2.4. Potential dust sources and source rocks

Besides the semi-arid and arid coastal areas of Peru and northern Chile, the Atacama Desert and the Altiplano Plateau (15–22°S) with its Salars and desert clay soils are favorable for dust production. Dust exported from the Altiplano can directly be entrained in tropospheric winds (Maher et al., 2010). Dust storms and dust devils are frequent there as well as around Iquique (20°S) at the Chilean coast (Goudie and Middleton, 2006; Kurgansky et al., 2010). Other acknowledged sources are reactivated desert dunes that have been produced under former drier conditions when clay aggregates were deposited during their formation or through post-depositional weathering (Goudie and Middleton, 2006; Pye, 1987). Such dunes are widespread in southern Peru and northern Chile (Howard, 1985). They provide silt and clay in substantial quantities, which can be entrained in the southeast trade winds during dust storms.

## 3. Materials and methods

The surface sediment material was sampled at the Oregon State University Marine Geology Repository. It was originally obtained during 16 different cruises to the tropical (south-)east Pacific between 1969 and 2000 (S2). We assume all samples to be of late Holocene age from results of isotope measurements on foraminifera (Rincón Martínez et al., 2010, in review), and because only the uppermost 2 cm were used for analyses. Grain-size distributions and clay-mineral compositions were analyzed on 75 and 70 samples, respectively. The samples were washed through a 63 μm mesh for foraminiferal studies published elsewhere (Rincón Martínez et al., in review). Organic carbon and calcium carbonate ($CaCO_3$) were removed from the fine fraction (<63 μm) with a 10% hydrogen peroxide ($H_2O_2$) solution and a 10% acetic acid ($H_3C$–COOH) solution, respectively. The silt (2–63 μm) and clay (≤2 μm) fractions were separated using the Atterberg settling method (Ehrmann et al., 1992).

We measured the grain-size distribution of the siliciclastic silt fraction with a Beckman-Coulter laser particle sizer. Besides organic matter and calcium carbonates, biogenic opal was removed boiling the samples with excess NaOH for 10 min. Microscope analyses confirmed that this method successfully removed all biogenic components. Shortly before the analysis, a few mg of $NaPyPO_4$ were added and brought to boil in order to avoid coagulation of particles. In order to prevent a bias caused by a different scattering behavior of elongated (or other shaped) particles, grain-size measurements with a laser particle sizer lasted 90 s each, during which the sample suspension was continuously pumped through the lens.

For clay-mineral composition analyses, the clay fraction was homogenized in an agate mortar. 40 mg of each sample together with an internal standard (1 ml of 0.4% molybdenite suspension ($MoS_2$)) were re-suspended for more consistent semi-quantitative measurements. Vacuum filtration of the suspension on membrane filters produced texturally oriented clay films with thicknesses of 50 to 100 μm (Petschick et al., 1996), which were then dried and transferred onto aluminum platelets (see Ehrmann et al., 1992). The samples were measured with CoKα-radiation (40 kV, 40 mA; $\lambda = 1.79$ Å) on a Philips PW 1710 goniometer equipped with an automatic divergence slit, and a graphite monochromator. To identify overlapping (clay) mineral peaks such as smectite and chlorite, the samples were glycolated at 60 °C for at least 12 h with the effect of widening the basal distance of smectite to 17 Å (Tucker, 1996) and measured from 2 to 40° 2θ with a step size of 0.02° 2θ. To distinguish the (002) kaolinite (3.58 Å) and (004) chlorite peaks (3.54 Å), the area between 28° and 30.5° 2θ was additionally scanned with steps of 0.005° 2θ. The diffractograms were later processed with the graphically based Macintosh Apple computer program "MacDiff 4.2.5" (Petschick et al., 1996, available at http://www.geologie.uni-frankfurt.de/Staff/Homepages/Petschick/Classicsoftware.html).

The relative clay-mineral contents (rel%) of illite, smectite, chlorite and kaolinite were determined semi-quantitatively by calculating the integrated peak areas of the clay-mineral basal reflections, weighted with the empirically determined factors after Biscaye (1964, 1965). These factors were used to ensure comparability with previous research (Lamy et al., 1999; Petschick et al., 1996).

Despite of several former studies (Dauphin, 1983; Molina-Cruz and Price, 1977; Prospero and Bonatti, 1969) that already considered the quartz content in SE Pacific sediments as an indicator for eolian-derived material, we also investigated the quartz and feldspar distributions in the clay fraction, which represent two noteworthy components of southeast Pacific sediments containing valuable information. We built the ratios of the peak area of each of the considered (clay)-minerals to the sum of all peak areas, assuming them to represent 100%. Quartz contents are generally low in the clay fraction due to the presence of clay minerals.

### 3.1. Statistical analysis

We applied the end-member modeling algorithm (EMMA) of Weltje (1997) to the siliciclastic grain-size data set in order to identify the original sediment populations that contribute to the terrigenous fraction of surface sediments. The minimum number of end members needed to model the variance in the data set satisfactorily is determined by the coefficients of determination for several different models. This 'goodness of fit' is calculated for each size class and represents the squared correlation coefficient ($r^2$) of the input variables and their approximated values (Prins and Weltje, 1999; Weltje, 1997).

For a more comprehensive understanding of the sediment provenance, we performed a K-means cluster analysis on the Biscay-factor weighted clay-mineral assemblage data. This allows a more precise characterization of the source areas, as the composition of the cluster center ideally represents an approximation of the source material composition. The clay-mineral assemblage data is a compositional data set, summing to 100%. To carry out multivariate statistical analyses, this data set has to be transformed to a vector space structure applying a log-ratio (Pawlowsky-Glahn and Egozcue, 2006 and references therein). In case of a K-means cluster analysis, the transformation of choice is a centered log-ratio. Different cluster configurations (2 to 10 clusters) were calculated with 100 replicates each. In order to obtain the optimal number of interpretable clusters, we calculated the Davies–Bouldin Index (Davies and Bouldin, 1979). The lower the index, the more compact are the clusters and the greater are the distances between the cluster centers. Starting with the least number of clusters, the first local minimum of the index thus represents the cluster number of choice. Each sample belongs to only one cluster.

## 4. Results

A first rough grain-size analysis, separating the lithogenic silt and clay fractions with the Atterberg settling method resulted in higher silt contents close to the South American continent. Silt/clay ratios exceed 2.0 even west of the Peru/Chile Trench. The silt content decreases with increasing distance from the coast in the Peru Basin but remains high around Carnegie Ridge and the Galapagos Islands (Fig. 3). Grain-size analysis of the silt fraction with a laser particle sizer resulted in grain-size distributions of 0.4 μm to, at most, 96.5 μm in 60 size classes. Even though the samples were sieved with a 63 μm mesh, up to three size classes larger than the cut-off value were measured due to elongated shapes of the particles that fit through the mesh, while the idealized spheric shapes do not. Grain-size distributions turned out to be polymodal, but always displayed one dominating mode. If 'mode' or 'modal grain-size' is not specified, we always refer to the dominant modes of the grain-size distributions. The minor modes are residues of the end-member analysis and not of interest here. Modal grain-size of the dominant modes varies between 4.05 and 60.5 μm, with offshore fining trends in the Peru Basin, while there is no trend visible north of the equator and extremely high values (up to >24 μm) around the Galapagos Islands, Carnegie Ridge and Galapagos Rise (Fig. 3). Finest sediments are found in the deepest areas of the central Peru Basin, with medians of 4.4 μm and less (not shown). Grain-size analyses of a few sediment samples including all size fractions to test the validity of silt representing the eolian-derived sediment fraction resulted in comparable distributions (S4), with the dominant modes ranging between 2 and 5 μm. The fraction >63 μm that remained after dissolution of carbonate, biogenic opal and organic carbon is composed of volcanic glass and/or authigenic particles, but not of terrigenous sand, and therefore does not influence our inferences about terrigenous sediments transported to the ocean.

For the end-member model the number of input variables, i.e. the number of size classes, was reduced to 58, due to the general fine-grained nature of the sediments. According to the results for the

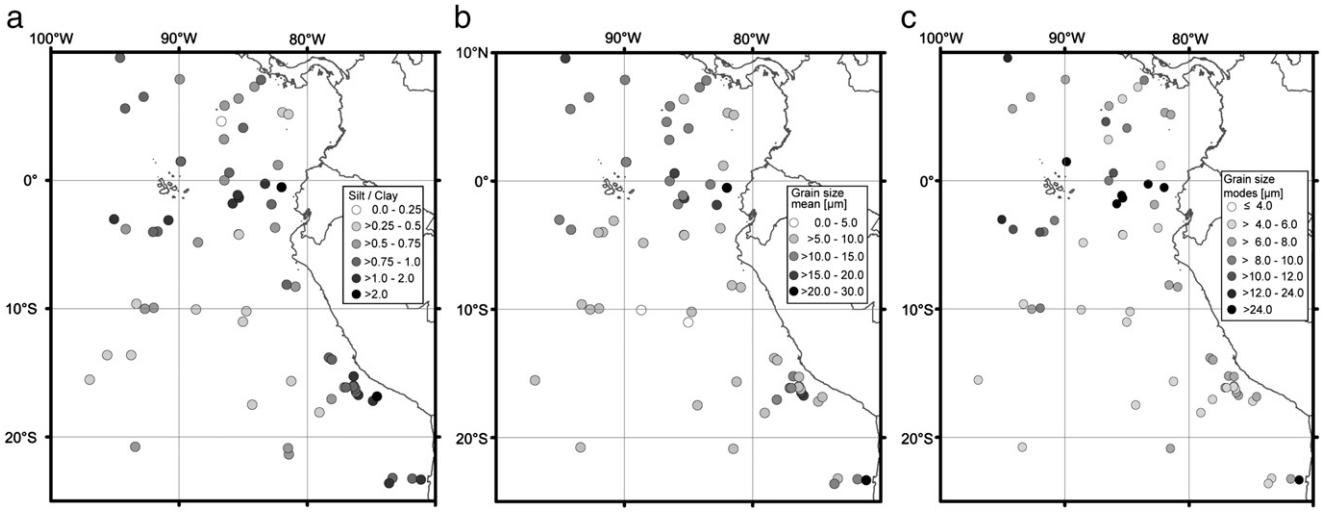


**Fig. 3.** Grain size analyses. a Siliciclastic silt/clay ratio of weight percentages from Atterberg settling method. South of 5°S considerably more silt is present a few hundred kilometers off the coast of South America, west of the Peru–Chile Trench, decreasing towards the open ocean. Elevated values around Carnegie Ridge and the Galapagos Islands are attributed to submarine volcanic debris. b Grain-size means show an overall picture comparable to the silt/clay ratio. North of the equator means vary around 10–15 μm, being of different sources and input mechanisms. c Highest modes are again found around Carnegie Ridge, mainly representing submarine volcanic glass.

coefficients of determination we determined the 4 end-member model to best approximate our data (Fig. 4). Fig. 4 displays the grain-size classes plotted against the coefficients of determination. The models with 2 and 3 end-members show a weak approximation $r^2$ (<0.6) of grain-sizes between 20 and 30 μm. The 4 end-member model is the one of choice because it reproduces the data well, with a mean coefficient of determination of $r^2 = 0.88$, still comprising an interpretable number of end members (EM) (Fig. 4). Fig. 5 shows the four end members, i.e., the distributions of the original grain-size populations (Fig. 5a), as well as their proportions (Fig. 5b–e), which, in sum, approximate the measured grain-size distribution of each sample. EM1 represents nearly all the samples in the central Peru Basin and the most western locations on Nazca Ridge (proportions of 0.8–1). It is the finest of the four end members with a dominant mode of 4.88 μm. EM2 largely overlaps with EM1, but has a distinctly coarser dominant mode of 5.88 μm. It shows the largest proportions in the locations closest to South America — also in the Panama Basin, and on and around the Galapagos Rise. The most distinct and the coarsest of all is EM3, being confined to the Carnegie Ridge and northwest of the Galapagos Islands. Like EM2, EM4 does not show a clear pattern north of the equator but concentrates around the ridges and the Galapagos Islands. These end members overlap considerably in their peak area, but have distinctly different dominant modes, of 5.88 and 9.37 μm, respectively (Fig. 5a).

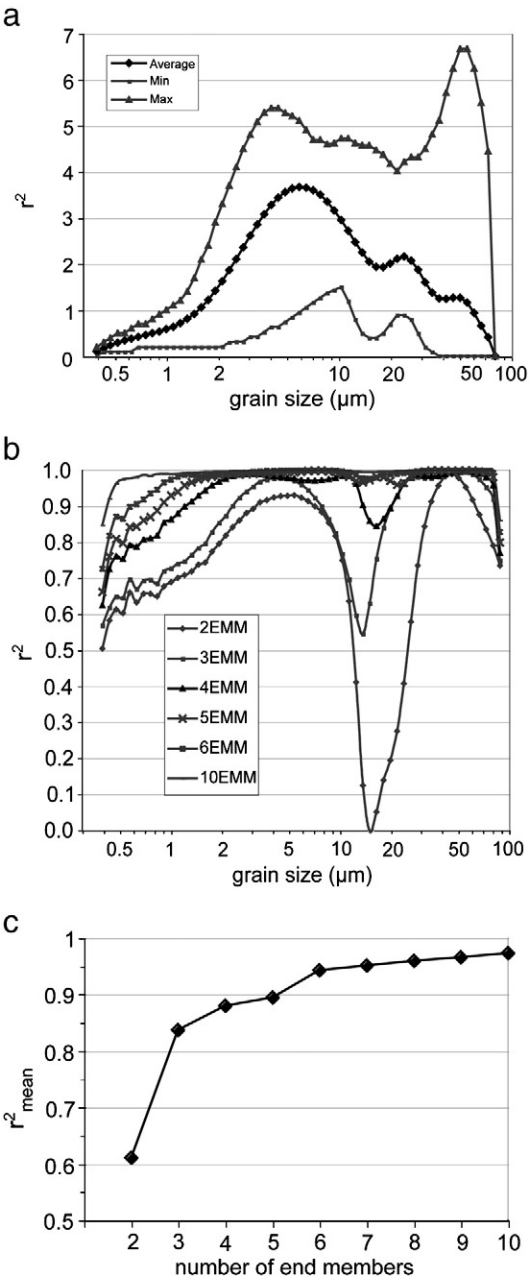


**Fig. 4.** End-member modeling results of surface sediment samples. (a) Summary statistics of input data (grain-size distributions, $n = 75$), maximum, mean and minimum frequency recorded in each size class; (b) coefficients of determination ($r^2$) for each size class of model with 2–10 end members; and (c) mean coefficient of determination ($r^2$) of all size classes for each end-member model.

Quartz, plagioclase and K-feldspar contents in the clay fraction all decrease from the Nazca Ridge towards the Carnegie Ridge, pointing to southeastern terrigenous sources (Fig. 6). In our study, lowest quartz contents (<3%) appeared north of about ~5°S with two exceptions on Cocos Ridge (4.6°N, 86.7°W) and just north of the Carnegie Ridge (0.6°N, 86.09°W). Even though generally very low in the clay fraction, Plagioclase and quartz both revealed relatively high values on Galapagos Rise.

Considering the four major clay-mineral groups, i.e., smectite, illite, chlorite and kaolinite, and applying the factor weighting after Biscaye (1965), our analyses mostly corroborate global clay-mineral compositions of recent ocean sediments, with the exception of kaolinite (Chamley, 1989) (Fig. 7). Smectite is by far the most abundant clay mineral in the whole study area, with contents spanning from 35% in the south to up to 97.5% around the Galapagos Islands and on the Carnegie Ridge. Contents are elevated along the Galapagos Rise, but low in the central Peru Basin and on the Nazca Ridge. Values from 55% to 85% north of the equator point to an additional source located between 5° and 10°N.

Illite, in contrast, is most abundant in the southern half of the study area, decreasing in a north-northwestern direction (Fig. 7a). Values reach up to 25% off Peru and on the Nazca Ridge in the southeast. Lowest contents have been recorded in the Panama Basin.

Chlorite points towards the same source areas as illite, although its distribution pattern is less well defined and constrained further to the south. It is the second most abundant clay-mineral group with values spanning from 0% south of the Galapagos Islands to 32% on Nazca Ridge. In contrast to illite, there is a source of chlorite in central America, as elevated contents of >20% have been recorded on the Cocos Ridge, while chlorite is not present around the Galapagos Islands and the Carnegie Ridge (Fig. 7c). Kaolinite does not show the typical distribution connected to extensive chemical weathering expected in tropical areas (Chamley, 1989). It depicts a patchy pattern without any distinct areas as the other mineral groups. Kaolinite reaches contents of >15% on the Galapagos Rise, north of the Galapagos Islands and the southern end of the Nazca Ridge, suggesting submarine sources there (Fig. 7d).

The Davies–Bouldin Index that we used as goodness of fit statistics for the K-means cluster analysis (S5) of the clay-mineral composition data suggests 4 clusters to best represent the data with a minimum number of clusters. Fig. 8 shows the four cluster centers. Cluster 1 represents surface sediments from the Nazca Ridge and the Peru Basin and possibly also offshore northern Chile, where samples are scarce. Its cluster center comprises relatively high contents of illite and chlorite, while smectite is reduced to 53%. By contrast, cluster center 2 is largely dominated by smectite (84%) while the other three clay mineral groups are almost negligible. Samples clustering around this center are confined to the Carnegie Ridge and the Galapagos Islands. It is closest in composition to cluster center 4, which differs mainly in its much higher content of chlorite (16%). Its spatial distribution is confined to the Panama Basin. Cluster center 3 is characterized by its relatively large contents of kaolinite (17%) and illite (15%). It is the least confined cluster, including patches of sediment samples on the northern and southern rims of the Carnegie Ridge and most samples from the Galapagos Rise as well as one single sample off southern Peru.

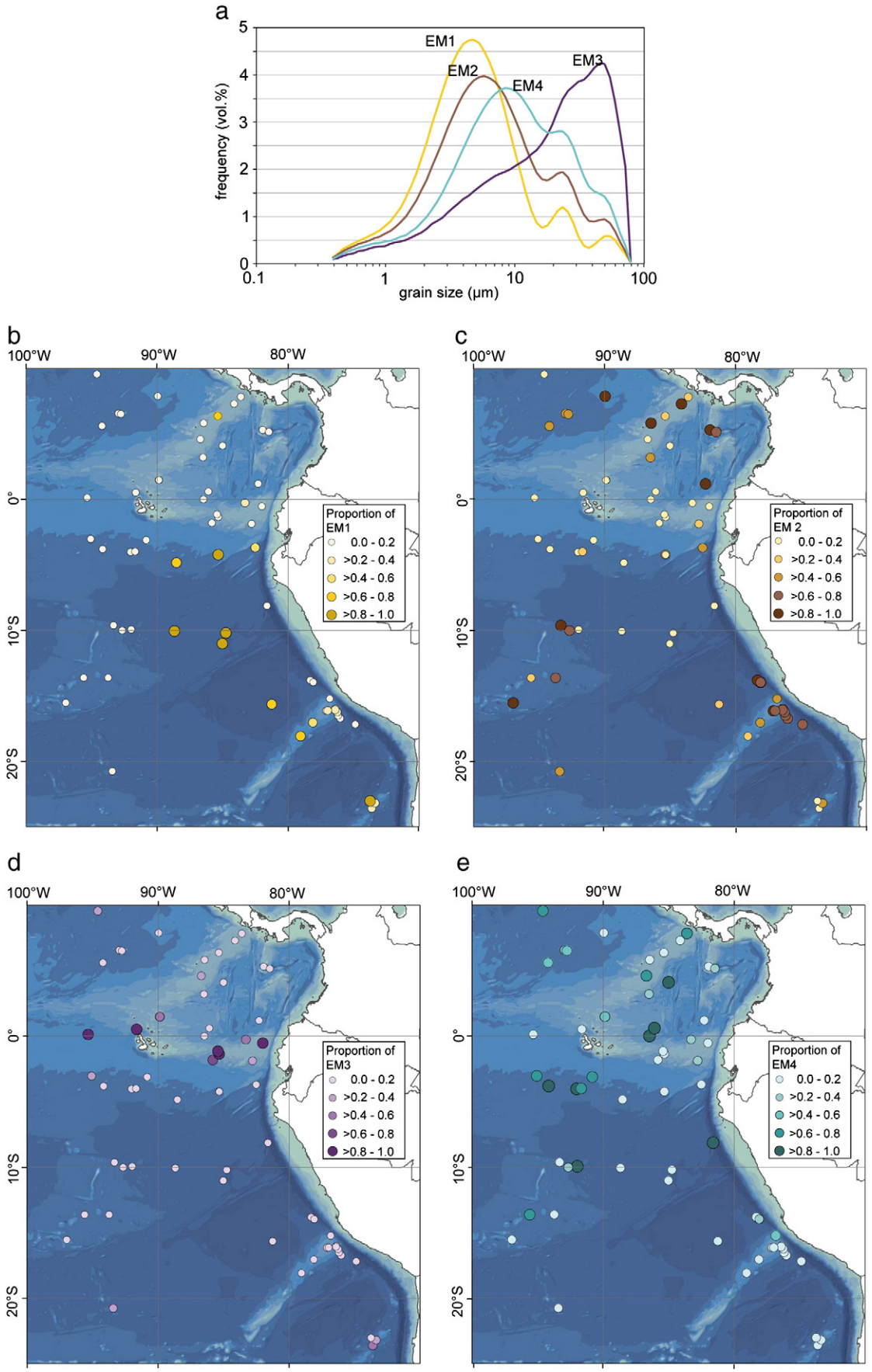


**Fig. 5.** Modeled end members of the terrigenous silt fraction from the southeast Pacific. (a) grain-size distributions of the 4 end members; and (b–e) spatial distribution of the proportions of each end-member.

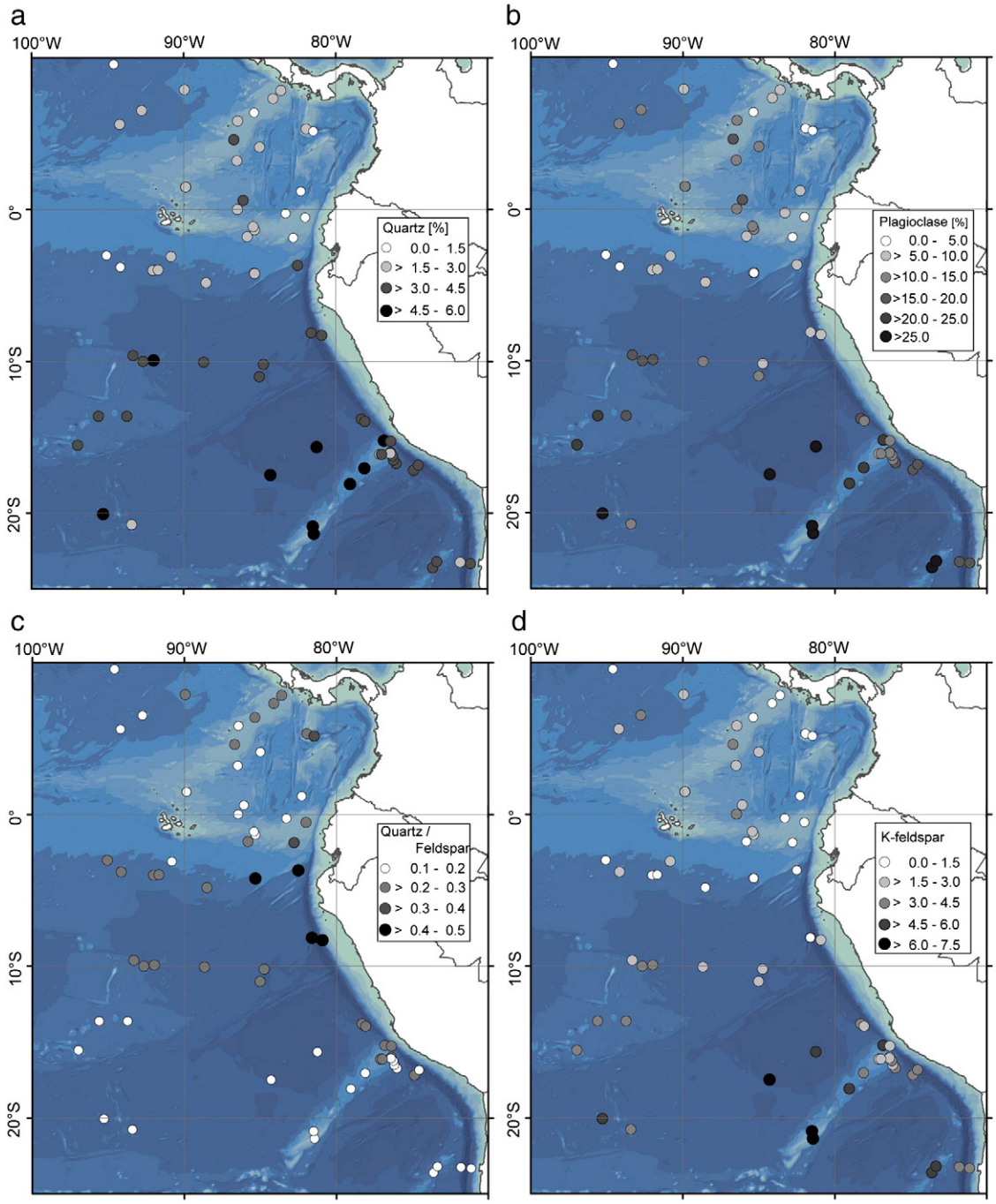


**Fig. 6.** Quartz and feldspar contents in the clay fraction of the surface sediment samples. (a) Quartz; (b) plagioclase; (c) quartz/feldspar ratio; and (d) k-feldspar.

## 5. Discussion

Dust plumes in the atmosphere above the southeast Pacific are rarely caught on satellite images (http://visibleearth.nasa.gov/view_rec.php?id=999), and haze recordings more than a few hundred kilometers offshore are sparse (Prospero and Bonatti, 1969). Nevertheless, because of the results of clay mineralogical analyses and the fine-grained nature of our sediment samples (see below), we believe that our results for recent sediments from west of the Peru–Chile Trench south of ~5°S solely depict eolian dust from the coastal deserts of Peru, but do not incorporate fluvial input signals. First of all, there are no major rivers to be found in the arid areas of South America. Macharé and Ortlieb (1992) found evidence for eolian deflation – not precipitation and runoff – to be the dominant erosive agent at the central coast of Peru. The existing streams are short and mainly transport coarse debris (Dunne and Mertes, 2007; Potter, 1994). Second, the Peru–Chile Trench forms a physiographic barrier, catching the majority of fluvial sediments. The little fluvial material transported offshore in nepheloid layers is outweighed by the eolian-derived sediment component (Krissek et al., 1980; Scheidegger and Krissek, 1982).

### 5.1. The provenance of dust in SE Pacific sediments

The lobes formed by the quartz, illite, chlorite, and – more southern – the plagioclase distribution (Figs. 6 and 7) and their decreasing tendencies from south(east) to north(west) in our study area reflect the major wind field of the SE trade winds and point to

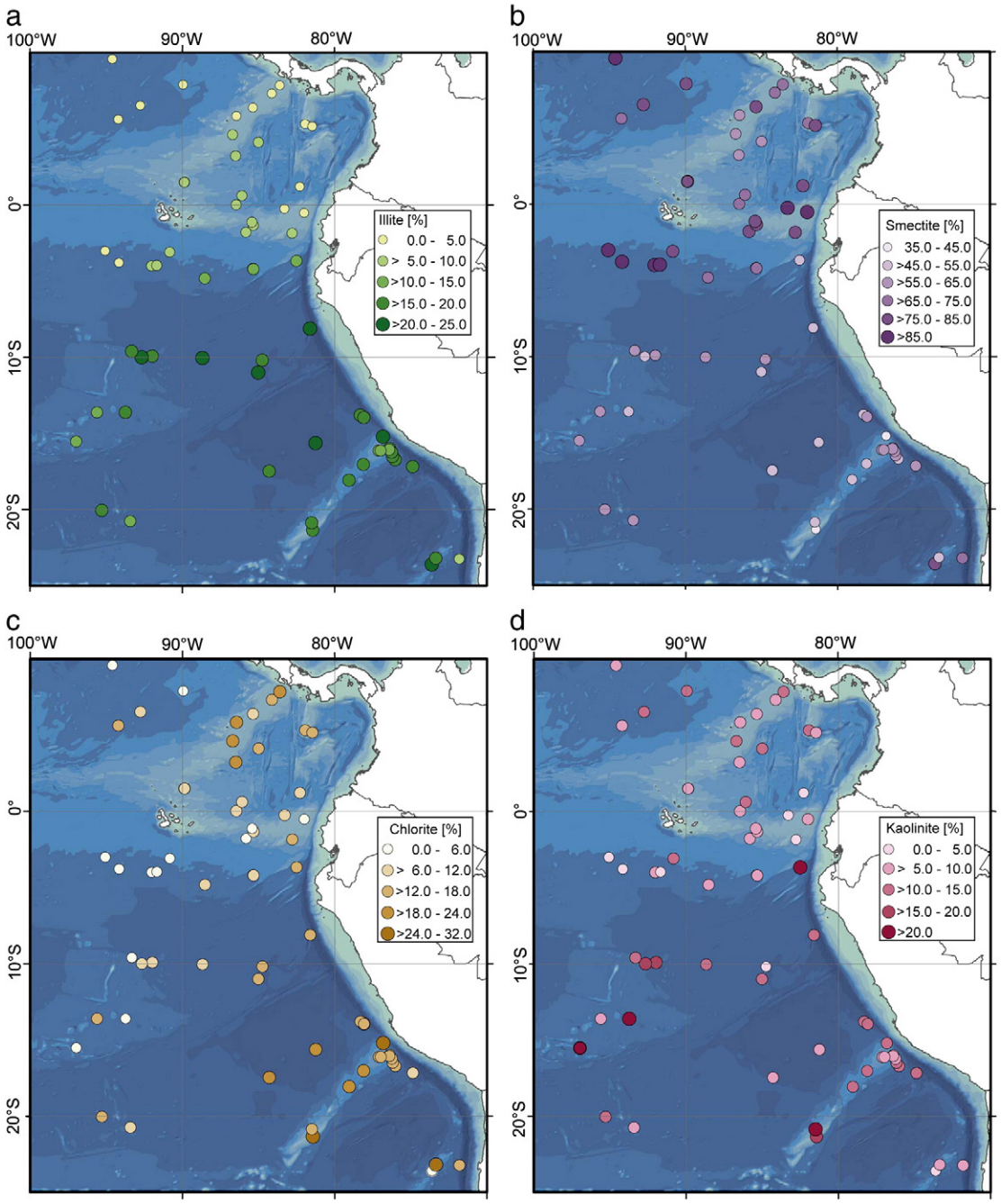


**Fig. 7.** Clay-mineral distributions in the southeast Pacific: (a–d) contents (%) of (a) illite, (b) smectite, (c) chlorite, and (d) kaolinite in the clay fractions.

them as the major agent of transport of terrigenous material (compare Figs. 2, 6 and 7). Prospero and Bonatti (1969) found quartz to be the prevalent mineral in atmospheric dust collected in the northern Peru basin, followed by plagioclase, muscovites (i.e., illites), smectites and chlorites. Flores-Aqueveque et al. (2009) also determined quartz and feldspars as the prevalent minerals in sands of the coastal desert of northern Chile. This corresponds to our findings (Figs. 6 and 7). The sources and transport pathways of the terrigenous components deposited on the Nazca Ridge and in the Peru Basin, are to be distinguished into two separate areas latitudinally. This difference is not as clearly visible in the grain-size distributions, nor shown in previous studies (e.g., Dauphin, 1983; Molina-Cruz and Price, 1977) using quartz contents to represent patterns of terrigenous input. Quartz, feldspars and illite are all products of physical weathering as typical for arid areas, and are among the main components of desert dust (e.g., Flores-Aqueveque et al., 2010). From modeling studies (e.g., Tanaka and Chiba, 2006) we know that the Peruvian coasts, the arid inland areas of southern Peru, the coastal areas of Chile and the semi-arid areas along the western Andean foothills are potential sources of dust. While both source areas, the northern/central Peruvian coast and the Atacama/Altiplano region further south, deliver quartz to our study area, highest quartz contents on the Nazca Ridge and in the southern Peru Basin a few hundred kilometers offshore point to the southern area as the stronger source. Closer to the coast smectite derived from the volcanic chain, restarting in the latitude of the Nazca Ridge, dilutes the quartz signal. The general decreasing trend of quartz contents in a north-northwestern direction was not recognized in the study of Molina-Cruz and Price (1977), which includes samples from the continental margin, and thus fluvial material, overprinting the eolian signal. Scheidegger and

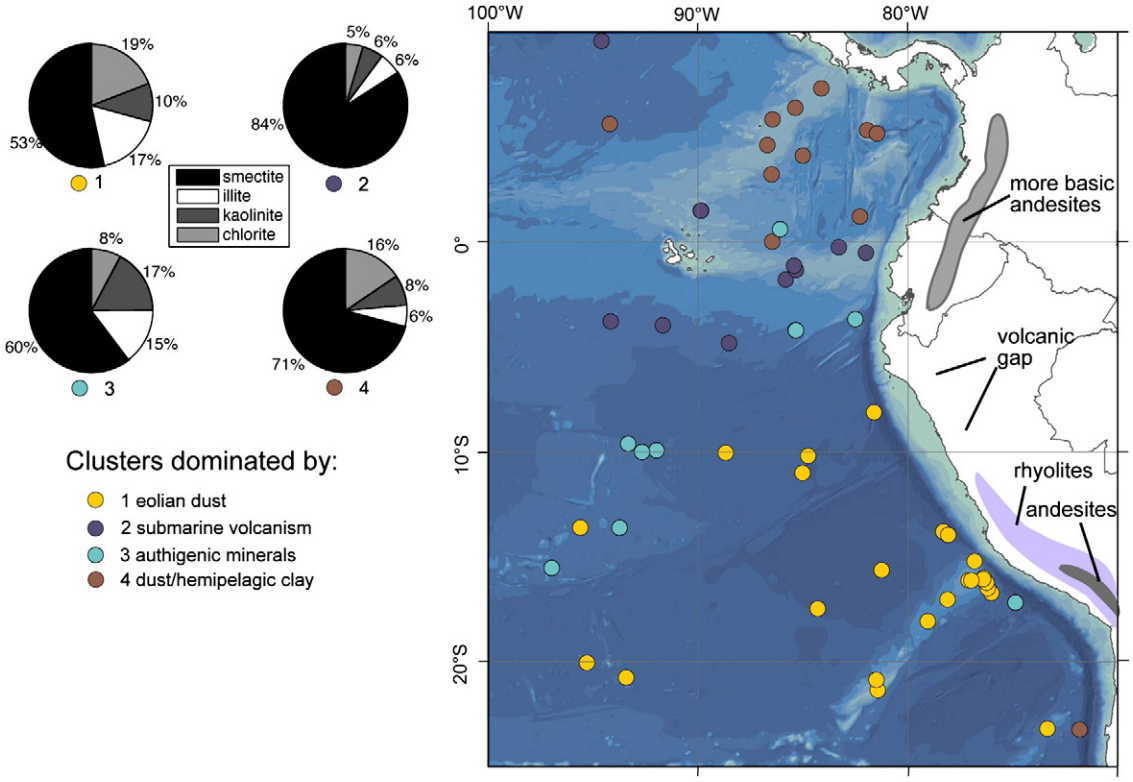


**Fig. 8.** K-means cluster analysis of clay-mineral distributions (rel.%), identifying four clusters. The compositions of the four cluster centers and their attributed meaning are shown on the left.
Indication of geological provinces are taken from Zeil, 1986.

Krissek (1982) found latitudinal geological differences mirrored in the quartz/plagioclase ratio of marine surface sediments. We confirm the higher quartz/feldspar ratios off northern Peru due to reduced amounts of plagioclase but also K-feldspars north of ~15°S. However, we cannot detect a similarity of dispersal patterns of (clay)-minerals or grain-size distributions to surface current patterns, diverted west off northern Chile/southern Peru and northwest off central/northern Peru, in our data as suggested by Scheidegger and Krissek (1982). Instead, the north-northwest trending lobes of quartz, illite and plagioclase (Figs. 6a and b, 7a) in our opinion reflect the distribution of dust via the main wind field of the trade winds. However, we have also detected eolian input from the central Peruvian coastal deserts in a western direction. As mentioned above, easterlies are prevalent around 7–8°S from June–October, suggesting eolian transport off northern Peru in a westerly direction, and a northwesterly direction from the Atacama Desert, contrasting the interpretation of Scheidegger and Krissek (1982). The major differences of the two source areas, i.e., the coastal desert of Peru and the Atacama Desert in northern Chile, are the amounts of feldspars and chlorite (Figs. 6 and 7). Quartz and feldspars are products of weathered volcanic rocks as well as physically weathered metamorphic rocks and are delivered from both source areas. However, feldspar weathers much faster than quartz and is usually an indicator of freshly weathered source rocks. It is reduced off northern Peru where the source rocks are mainly granitic intrusives instead of freshly weathered basaltic and gabbroic rocks. Especially weathered andesites deliver high amounts of plagioclase (Fig. 6b) (cf. Scheidegger and Krissek, 1982). Its absence offshore north–central Peru corresponds to the gap in the volcanic chain of the Andean Cordillera (Orme, 2007; Zeil, 1986). Ignoring the sub-aqueous sources of plagioclase (see below), the spatial distributions of feldspars display a decreasing trend in north-northwestern direction and thus point toward the southern source in northern Chile (cf. Stuut et al., 2006). As a consequence, the ratio of quartz/feldspars depicts a dust plume extending from the coastal desert of Peru north of ~15°S (Fig. 6c) as it was presented by Molina-Cruz and Price (1977).

In contrast to Scheidegger and Krissek (1982) who refer to the findings of Rosato and Kulm (1981) on clay-mineral abundances, we do think clay-mineral composition is a sensitive indicator of dispersal patterns providing information for the entire study area, not just for the continental margin. Besides, the study area of Rosato and Kulm (1981) is considerably smaller than ours, focusing on sediment input from central Peru only. They did not relate their data to specific geologic provinces. Like quartz (Leinen et al., 1986), illite is a robust indicator of dust in the South Pacific (Windom, 1976). It strongly supports the hypothesis of dust entrainment from the semi- and hyperarid coastal areas and the Atacama Desert as inferred from the quartz distribution of this study. Our findings of 20–25% of illite around the Nazca Ridge agree well with the average illite concentration in all of the South Pacific of 26% (Windom, 1976), but disagree with the findings of Rosato and Kulm (1981) who detected illite contents of 30–50% in the Peru Basin. In contrast to quartz, illite contents are as high off northern Peru as off southern Peru (Figs. 6a and 7a) as it is derived from the desert dust and omnipresent weathered metamorphic rocks, and the outcropping Precambrian basement of the Coastal Cordillera. Unlike the feldspars or quartz, which decrease off central and northern Peru, it is not a product of Quaternary volcanic rocks that are absent between 2°S and 15°S due to the volcanic gap. Illite continuously decreases in a northern direction, even across the equator. This indicates dust transport from the southern source areas at least as far north as the austral summer position of the ITCZ.

Like quartz, chlorite displays highest contents further offshore on Nazca Ridge and in the southern Peru Basin rather than closer to the coast, indicating its southern origin. It points to a major source in the granites of southern Peru and the Atacama Desert in northern Chile. This interpretation differs from Rosato and Kulm (1981) who

attribute the main source to the coastal batholith of Peru due to highest chlorite values on the continental margin.

In our results of the k-means cluster analysis, which allocates each sample to only one cluster center, the southern samples all cluster around center 1, which includes the highest illite and chlorite contents of all clusters, adding up to 36%. Inferred from the composition of this cluster center, this represents the dust-dominated sedimentation part of our study area (Fig. 8). It comprises the area of influence of both major dust source areas, the Nazca Ridge and the Peru Basin, extending onto the Galapagos Rise. This is also the area where the ubiquitous but much less abundant smectite originating from freshly weathered volcanic rock is obviously diluted by the other mineral groups. Kaolinite is highly variable (cf. Rosato and Kulm, 1981) in this area and therefore does not contribute to the characterization of its sediments.

Sediments from the Galapagos Rise also contain dust derived from the arid areas of Peru and Chile (see above and Figs. 6a and b, 7a), but are highly influenced by authigenic particle formation. They mainly cluster around cluster center 3, which displays rather high contents of kaolinite, typical of submarine weathering of k-feldspars (Rex and Martin, 1966) but still considerable amounts of illite from eolian input. High values of quartz and plagioclase on the Galapagos Rise, however, can be attributed to submarine volcanic activity, rather than to eolian input (Bonatti and Arrhenius, 1970; Byerly et al., 1976; Peterson and Goldberg, 1962; Wright, 2004).

### 5.2. The eolian signal on Nazca Ridge and the Peru Basin

Eolian mineral dust grain-sizes in the SE Pacific are smaller than those found in the major dust study areas such as off West Africa (Fig. 3 this study; Dauphin, 1983; Stuut et al., 2005), but comparable in size to those found in northern Pacific sediments (medians of ~3–8 μm (Rea and Hovan, 1995)). This is because most of the dust transported to the southeastern Pacific is not injected into the higher atmosphere but incorporated into the low level trade winds (Dauphin, 1983) and larger dust grains (>20 μm) are removed quickly due to gravitational fallout when transported offshore (Prospero and Bonatti, 1969). We attribute the two end-members with the finest dominant modes to eolian input to our study area (Fig. 5). EM1 represents nothing but eolian dust. It is spatially distributed in the Peru Basin with a constant distance from the South American coast as it represents the fine dust component sorted along its transportation path by gravitational fallout, as already suggested by Prospero and Bonatti (1969). The fine mode of EM1 (4.88 μm) agrees well with the modes of grain-size analyses of dust collected from the atmosphere by Prospero and Bonatti. During their dust collection study in the equatorial east Pacific, they determined dominant modal grain-sizes of 2–5 μm for single dust collections southwest of the Galapagos Islands (downwind in our study area) with a particle settling technique. The findings of Dauphin (1983) for quartz grain-sizes from the Peru Basin match our results very well, even though we investigated the complete lithogenic silt fraction. Results from Dauphin show grain-size modes of 7–8 Φ for the Peru Basin, corresponding to 4–8 μm in our study (Fig. 3). By contrast, mean grain-sizes are coarser in our study area than dust collected south of 25°S (2.3 μm at 30°S (Wagener et al., 2008)). This difference marks the southern boundary of the dust pathways from the western South American deserts via the Southeast Trade winds.

The mapped proportions of EM1 (Fig. 5) are noticeably uniform in the deepest parts of the Peru Basin, all samples being equally well represented by this end member (proportions of 0.8–1). The uniformity in grain-size distribution is attributed to subsequent redistribution by bottom nepheloid layers in the basin as stated by Krissek et al. (1980). EM2 in our opinion is not a real end member but incorporates two different sediment populations that can be distinguished due to their geographical distribution: It approximates well most samples close to the South American continent between 3°S and 20°S and between 10°N and 0°. Combined with EM1, this represents the eolian input from the coastal deserts in Peru and the Atacama Desert in northern Chile, exhibiting a fining trend towards the open ocean. North of the equator the presence of EM2 suggests wet deposited dust in the doldrums (Fig. 5). The grain-size distributions of sediments from the Panama Basin represented by EMs 2 and 4 are a consequence of interfering transport agents and source areas. Some dust is transported via the Trade winds from Ecuador and northern Peru when it turns into a northeasterly direction offshore Ecuador. Prospero and Bonatti (1969) identified a dust source in the arid regions of western and southern Mexico for the northwestern Panama Basin. However, strong bottom water currents and thus sediment redistribution (Heath et al., 1974) play a major role in the redistribution of sediments (Lonsdale, 1976). Eolian input to the Panama Basin will be discussed in more detail later.

The seven samples retrieved from the Galapagos Rise are exceptional in their grain-size distribution as well as in all other proxies investigated. Sediments do not consist mainly of dust and biogenic opal and/or carbonate as sediments from Peru Basin, but are largely limited to authigenic particle formation at the ultra-slow spreading ridge (Wright, 2004), such as iron-manganese oxides or quartz and feldspars (cf. Bonatti and Arrhenius, 1970; Byerly et al., 1976). This makes their grain-size distributions exceptionally coarse. EM2 and EM4 best approximate grain-sizes in the area of the Galapagos Rise, since together they comprise the whole unsorted silt fraction of 2–63 μm. We thus corroborate the study of Krissek et al. (1980) who found considerable amounts of sand and silt-sized material in sediments from the Galapagos Rise originating from hydrothermal processes.

### 5.3. Terrigenous input to the Carnegie Ridge and the Panama Basin

As mentioned above, our illite data indicate dust transported as far north as 5°N with the major wind field of the Trade winds (Figs. 2 and 7). This observation could not be resolved with the grain-size data. EM3, characteristic for sediments around the Galapagos Islands and Carnegie Ridge, together with EM4 represents very coarse-grained volcanic glass originating from the Galapagos Islands. It is the area of the highest smectite values that are fed by different sources. Wet chemical weathering of volcanic rocks and basic submarine volcanism are generally known to produce major amounts of smectite (Chamley, 1989). As precipitation and thus wet chemical weathering as well as continental and submarine volcanism are omnipresent in the area of the doldrums, so is smectite. Samples from the Carnegie Ridge and south of the Galapagos Islands thus cluster around cluster center 2 (average smectite content 84%) of the k-means cluster analysis (Fig. 8). The Equatorial Undercurrent (Strub et al., 1998) most likely distributes material from the Galapagos Islands to the east. Prospero and Bonatti (1969), however, found also considerable amounts of smectite in dust samples from northeast of the Galapagos Islands, which they related to semi-arid source areas in Ecuador and northern Peru. On the continent, the area dominated by cluster 2 corresponds to the area of extreme climatic contrasts with interchanging humid and arid conditions, i.e., wet-chemical weathering and (smectite-rich) dust production. The area experiences easterly winds in austral summer. The signal we retrieved from surface sediments very likely contains smectite from both windborne dust and submarine volcanic debris (cf. Heath et al., 1974), but also fluvial debris originating from the Gulf of Guayaquil on the eastern end of the Carnegie Ridge (Rincón Martínez et al., 2010). By contrast, dust samples from the atmosphere above the Panama Basin, the Cocos Ridge and the Guatemala Basin were dominated by plagioclase, pointing to a dust source in western and southern Mexico (Prospero and Bonatti, 1969). Our results for plagioclase also show increased values on the Cocos Ridge, but also across the saddle of the Carnegie Ridge. It is not clear, whether this reflects dust and/or submarine sources. Additionally, the quartz/feldspar ratio is increased

on the Cocos and Coiba ridges extending south from Central America. Smectite, and especially chlorite are also increased on the ridges.

During boreal winter, strong winds cross the Panama Isthmus. Dominant northeast trade winds result in decreasing rainfall from east to west in the northern parts, while the equatorial low causes extreme (unstable convective thunderstorm) precipitation within the ITCZ (Bundschuh et al., 2007). Dust transported across Central America from above the Atlantic might thus be a minor contributor to these signals (Liang et al., 2009; Prospero and Bonatti, 1969; Prospero and Lamb, 2003), but chlorite and most likely quartz seem to be related to a local source in Costa Rica. Inland of the Cocos Ridge, the Cordillera de Talamanca corresponds to a gap of the otherwise closely spaced Quaternary stratovolcanoes that are most likely sources of airborne smectite. The Cordillera de Talamanca, however, is interspersed with batholiths and granitoid intrusions (Abratis, 1998), and probably the provenance of quartz and chlorite. Despite the identification of the source area, we cannot prove the transport agent for these terrigenous sediments, which might be eolian as well as hemipelagic. After all, fluvial erosion is predominant due to heavy rainfalls in the doldrums (Bundschuh et al., 2007). According to Heath et al. (1974) fluvial input and further distribution by intermediate water currents are responsible for the increased chlorite contents on the ridges. Our k-means cluster analysis resulted in one cluster that is confined to Panama Basin. This cluster center 4 represents sediments relatively rich in chlorite, while smectites remain the predominant mineral group, emphasizing the dominant northern provenance of surface sediments in the Panama Basin.

## 6. Conclusions

Based on the clay-mineral and grain-size distribution data obtained from surface sediment samples from the southeast Pacific, the following conclusions can be drawn:

(1) Clay-mineral compositions of surface sediments allow the identification of different geological provenances also in offshore areas of the southeast Pacific. We were able to confine the smectite-dominated sedimentation areas to the continental areas influenced by extensive tropical rainfall related to the ITCZ. Furthermore, the smectite and plagioclase distributions in marine surface sediments mirror the volcanic gap between 2° and 15°S.
(2) The illite content in the clay fraction is a valuable indicator of dust supplied from the Atacama Desert as preserved in marine sediments in the SE Pacific.
(3) Wind is the major transport agent of terrigenous sediments west of the Peru–Chile Trench between 5°S and 25°S. Dust is distributed over the ocean by the southeast Trade winds.
(4) The Nazca Ridge receives considerable amounts of eolian-derived silt-sized material from the semi- and hyper-arid areas of South America and is therefore an area suitable for paleo-dust research.
(5) Different proxies are necessary to differentiate between hemipelagic and eolian sediment transport in the Panama Basin. Due to strong bottom water circulation overprinting the terrigenous supply to the basin we have not been able to identify transport agents satisfactorily.
(6) Areas of low sedimentation rates and authigenic particle production render the interpretation of end-member analysis results as presented here difficult, because some of the obtained end-members incorporate more than one original sediment population and are thus no true end-members by definition. Nevertheless, the area dominated by eolian-derived terrigenous supply was identified by combining the results of clay-mineral compositions and grain-size distribution of the surface sediments.

## Acknowledgements

We thank R. Fröhlking and S. Wiebe (AWI) for technical support in the lab and Hannes Schmidt for the clay-mineral sample preparation. We also thank D. Heslop (University of Bremen) for analytical support. Thomas Laepple kindly provided his expertise plotting the NCEP data. Core-top samples were provided by the Marine Geology Repository at the Oregon State University. We thank Bobbi Conrad and Alan Mix for support during sampling. Gert-Jan Weltje is acknowledged for providing the end-member modeling algorithm. The German Science Foundation financed this study within the project Ti 240/17 (DFG).

## Appendix A. Supplementary data

Supplementary data to this article can be found online at doi:10.1016/j.margeo.2010.12.006.

## References

Abratis, M., 1998. Geochemical Variations in Magmatic Rocks from Southern Costa Rica as a Consequence of Cocos Ridge Subduction and Uplift of the Cordillera de Talamanca. Universität Göttingen, Göttingen.
Arimoto, R., 2001. Eolian dust and climate: relationships to sources, tropospheric chemistry, transport and deposition. Earth Science Reviews 54 (1–3), 29.
Biscaye, P.E., 1964. Distinction between kaolinite and chlorite in recent sediments by X-ray diffraction. American Mineralogist 49, 1282–1289.
Biscaye, P.E., 1965. Mineralogy and sedimentation of recent deep-sea clay in the atlantic ocean and adjacent seas and oceans. Geological Society of America Bulletin 76 (7), 803–831.
Bonatti, E., Arrhenius, G., 1970. Acidic rocks on the pacific ocean floor. In: Maxwell, A.E. (Ed.), The Sea. Jon Wiley & Sons, New York, pp. 445–464.
Boven, K.L., Rea, D.K., 1998. Partitioning of eolian and hemipelagic sediment in eastern Equatorial Pacific core TR 163-31B and the late Quaternary paleoclimate of the Northern Andes. Journal of Sedimentary Research 68, 850–855.
Bruniard, E.D., 1982. La diagonal árida argentina: un límite climático real (The Argentinian arid diagonal: a real climatic boundary). Revista Geográfica Intituto Panamericano de Geografía e Historia 95, 5–20.
Bundschuh, J., Winograd, M., Michael, D., Alvarado, G.E., 2007. Regional overview. In: Bundschuh, J., Alvarado, G.E. (Eds.), Central America: Geology, Resources, and Hazards. Taylor & Francis/Balkema, Leiden, The Netherlands.
Byerly, G.R., Melson, W.G., Vogt, P.R., 1976. Rhyodacites, andesites, ferro-basalts and ocean tholeiites from the Galapagos spreading center. Earth and Planetary Science Letters 30, 215–221.
Chamley, H., 1989. Clay Sedimentology. Springer Verlag, Berlin. 623 pp.
Dauphin, J.P., 1983. Eolian Quartz Granulometry as a Paleowind Indicator in the Northeast Equatorial Atlantic, North Pacific and Southeast Equatorial Pacific, University of Rhode Island.
Davies, D., Bouldin, D., 1979. A cluster separation measure. IEEE Transactions on Pattern Analysis and Machine Intelligence PAMI-1, 224–227.
Dunne, T., Mertes, L., 2007. Rivers. In: Veblen, T.T., Young, K.R., Orme, A.R. (Eds.), The Physical Geography of South America. : Oxford regional environments series. Oxford University Press, Oxford.
Ehrmann, W.U., Melles, M., Kuhn, G., Grobe, H., 1992. Significance of clay-mineral assemblages in the Antarctic Ocean. Marine Geology 107 (4), 249–273.
Flores-Aqueveque, V., Vargas, G., Rutllant, J., Le Roux, J.P., 2009. Estacionalidad de la erosion y el transporte eólico de partículas en el desierto costero de Atacama, Chile (23°S). Andean Geology 36 (2), 288–310.
Flores-Aqueveque, V., Alfaro, S., Muñoz, R., Rutllant, J., Caquineau, S., Le Roux, J.P., Vargas, G., 2010. Aeolian erosion and sand transport over the Mejillones Pampa in the coastal Atacama Desert of northern Chile. Geomorphology 120 (3–4), 312–325.
Garreaud, R.D., Muñoz, R.C., 2005. The low-level jet off the west coast of subtropical South America: structure and variability. Monthly Weather Review 133, 2246–2261.
Garreaud, R., Vuille, M., Clement, A.C., 2003. The climate of the Altiplano: observed current conditions and mechanisms of past changes. Palaeogeography, Palaeoclimatology, Palaeoecology 194 (1–3), 5.
Goudie, A.S., Middleton, N.J., 2006. Desert Dust in the Global System. Springer, Heidelberg. 287 pp.
Harrison, S.P., Kohfeld, K.E., Roelandt, C., Claquin, T., 2001. The role of dust in climate changes today, at the last glacial maximum and in the future. Earth Science Reviews 54 (1–3), 43–80.
Heath, G.R., Moore, T.C., Roberts, G.L., 1974. Mineralogy of surface sediments from the Panama Basin, Eastern Equatorial Pacific. Journal of Geology 82 (2), 145–160.
Holz, C., Stuut, J.-B.W., Henrich, R., 2004. Terrigenous sedimentation processes along the continental margin off NW Africa: implications from grain-size analysis of seabed sediments. Sedimentology 51, 1145–1154.
Honjo, S., 1982. Seasonality and interaction of biogenic and lithogenic particulate flux at the panama basin. Science 218, 883–884.
Howard, A.D., 1985. Interaction of sand transport with topography and local winds in the Northern Peruvian desert. In: Barndorff-Nielsen, O.E., Moller, J.T., Romer

Rasmussen, K., Willetts, B.B. (Eds.), Workshop on the Physics of Blown Sand Memoirs. Department of Theoretical Statistics, Institute of Mathematics, University of Aarhus, Denmark, pp. 511–543.
Jickells, T.D., et al., 2005. Global iron connections between desert dust, ocean biogeochemistry, and climate. Science 308, 67–71.
Joussaume, S., 1990. Three-dimensional simulations of the atmospheric cycle of deser dust particles using a general circulation model. Journal of Geophysical Research 95 (D2), 1909–1941.
Kalnay, E., et al., 1996. The NCEP & NCAR 40-year reanalysis project. Bulletin of the American Meteorological Society 77 (3), 437–471.
Kessler, W.S., 2006. The circulation of the eastern tropical Pacific: a review. Progressive Oceanography 69 (2–4), 181–217.
Kienast, S.S., Kienast, M., Mix, A.C., Calvert, S.E., François, R., 2007. Thorium-230 normalized particle flux and sediment focusing in the Panama Basin region during the last 30,000 years. Paleoceanography 22, PA2213.
Krissek, L.A., Scheidegger, K.F., Kulm, L.D., 1980. Surface sediments of the Peru–Chile continental margin and the Nazca plate. Geological Society of America Bulletin 91 (6), 321–331.
Kurgansky, M., Montecinos, A., Metzger, S., Villagran, V., Verdejo, H., 2010. Filed study of atmospheric dust devils in the Atacama Desert. Geophysical Research Abstracts 12, EGU2010-1246, EGU General Assembly 2010.
Lamy, F., Hebbeln, D., Wefer, G., 1999. High-resolution marine record of climatic change in mid-latitude Chile during the last 28,000 years based on terrigenous sediment parameters. Quaternary Research 51, 83–93.
Leduc, G., Vidal, L., Cartapanis, O., Bard, E., 2009. Modes of eastern equatorial Pacific thermocline variability: implications for ENSO dynamics over the last glacial period. Paleoceanography 24, PA3202.
Leinen, M., Cwienk, D., Heath, G.R., Biscaye, P.E., Kolla, V., Thiede, J., Dauphin, J.P., 1986. Distribution of biogenic silica and quartz in recent deep-sea sediments. Geology 14 (3), 199–203.
Lettau, H., Costa, J.R., 1978. Characteristic winds and boundary layer meteorology of the arid zones in Peru and Chile. In: Lettau, H., Lettau, K. (Eds.), Exploring the World's Driest Climate. Center for Climatic Research, Madison, WI, pp. 163–181.
Li, F., Ginoux, P., Ramaswamy, V., 2008. Distribution, transport, and deposition of mineral dust in the Southern Ocean and Antarctica: contribution of major sources. Journal of Geophysical Research 113, D10207.
Liang, J.-H., McWilliams, J.C., Gruber, N., 2009. High-frequency response of the ocean to mountain gap winds in the northeastern tropical Pacifc. Journal of Geophysical Research 114 (C12005), 1–12.
Lonsdale, P., 1976. Abyssal circulation of the southeastern pacific and some geological implications. Journal of Geophysical Research 81 (6), 1163–1176.
Lonsdale, P., 1977. Inflow of bottom water to the Panama Basin. Deep-Sea Research 24, 1065–1101.
Lyle, M., Pisias, N., Paytan, A., Martinez, J.I., Mix, A., 2007. Reply to comment by R. Francois et al. on 'Do geochemical estimates of sediment focusing pass the sediment test in the equatorial Pacific?' Further explorations of 230Th normalization. Paleoceanography 22, PA1217.
Macharé, J., Ortlieb, L., 1992. Plio-quaternary vertical motions and the subduction of the Nazca Ridge, central coast of Peru. Tectonophysics 205 (1–3), 97.
Maher, B.A., Prospero, J.M., Mackie, D., Gaiero, D., Hesse, P.P., Balkanski, Y., 2010. Global connections between Aeolian dust, climate and ocean biogeochemistry at the present day and at the last glacial maximum. Earth Science Reviews 99, 61–97.
Molina-Cruz, A., Price, P., 1977. Distribution of opal and quartz on the ocean floor of the subtropical southeastern Pacific. Geology 5 (2), 81–84.
Nur and Ben-Avraham, 1981. Volcanic gaps and the consumption of aseismic ridges in South America. Geological Society of America Memoir 154, 729–740.
Orme, A.R., 2007. The tectonic framework of South America. In: Veblen, T.T., Young, K.R., Orme, A.R. (Eds.), The Physical Geography of South America. Oxford Regional Environments Series. Oxford University Press, Oxford.
Pawlowsky-Glahn, V., Egozcue, J.J., 2006. Compositional data and their analysis: an introduction. In: Buccianti, A., Mateu-Figueras, G., Pawlowsky-Glahn, V. (Eds.), Compositional Data Analysis in the Geosciences: from Theory to Practice. Geological Society, London, pp. 1–10.
Peterson, M.N.A., Goldberg, E.D., 1962. Feldspar distributions in South Pacific pelagic sediments. Journal of Geophysical Research 67 (9), 3477–3492.
Petschick, R., Kuhn, G., Gingele, F., 1996. Clay-mineral distribution in surface sediments of the South Atlantic: sources, transport, and relation to oceanography. Marine Geology 130 (3–4), 203–229.
Potter, P., 1994. Modern sands of South America: composition, provenance and global significance. Geologische Rundschau 83 (1), 212.
Prins, M.A., Weltje, G.J., 1999. End-member modelling of siliciclastic grain-size distributions: the late quaternary record of eolian and fluvial sediment supply to the Arabian Sea and its paleoclimatic significance. In: Harbaugh, J.W., et al. (Ed.), Numerical Experiments in Stratigraphy: Recent Advances in Stratigraphic and Sedimentologic Computer Simulations. : SEPM Special Publication. Geological Society Publishing House, London.
Prospero, J.M., Bonatti, E., 1969. Continental dust in the atmosphere of the eastern equatorial Pacific. Journal of Geophysical Research 74, 3362–3371.
Prospero, J.M., Lamb, P.J., 2003. African droughts and dust transport to the caribbean; climate change implications. Science 302, 1024–1027.
Prospero, J.M., Ginoux, P., Torres, O., Nicholson, S.E., Gill, T.E., 2002. Environmental characterization of global sources of atmospheric soil dust identified with the Nimbus 7 Total Ozone Mapping Spectrometer (TOMS) absorbing aerosol product. Review of Geophysics 40 (1), RG1002.
Pye, K., 1987. Aeolian Dust and Dust Deposits. Academic Press, London.
Rea, D.K., 1994. The paleoclimatic record provided by eolian deposition in the deep sea: the geologic history of wind. Review of Geophysics 32, 159–195.
Rea, D.K., Hovan, S.A., 1995. Grain-size distribution and depositional processes of the mineral component of abyssal sediments: lessons from the North Pacific. Paleoceanography 10 (2), 251–258.
Rex, R.W., Martin, B.D., 1966. Clay mineral formation in sea water by submarine weathering of K-feldspars. Clays Clay Mineralogy 14, 235–240.
Ridgwell, A.J., 2002. Dust in the Earth system: the biogeochemical linking of land, air and sea. Philosophical Transactions Mathematical Physical and Engineering Sciences 360, 2905–2924.
Rincón Martínez, D., Lamy, F., Contreras, S., Leduc, G., Bard, E., Saukel, C., Blanz, T., Mackensen, A., Tiedemann, R., 2010. More humid interglacials in Ecuador during the past 500 kyr linked to latitudinal shifts of the Equatorial Front and the Intertropical Convergence Zone in the eastern tropical Pacific. Paleoceanography 25, PA2210. doi:10.1029/2009PA001868.
Rincón Martínez, D., Steph, S., Lamy, F., Mix, A., Mackensen, A., Tiedemann, R., Tracking the Equatorial Front in the eastern equatorial Pacific Ocean by the isotopic and faunal composition of planktonic foraminifera. Marine Micropaleontology, in review.
Rosato, V.J., Kulm, L.D., 1981. Clay mineralogy of the Peru continental margin and adjacent Nazca plate: Implications for provenance, sea level changes, and continental accretion. In: Kulm, L.D., Dymond, J., Dasch, E.J., Hussong, D.M., Roderick, R. (Eds.), Nazca Plate: Crustal Formation and Andean Convergence: Geological Society of American Memoir, 154, pp. 545–568.
Rosato, V.J., Kulm, L.D., Derks, P.S., 1975. Surface sediments of the Nazca Plate. Pacific Science 29 (1), 117–130.
Rutllant, J., Fuenzalida, H., Aceituno, P., 2003. Climate dynamics along the arid northern coast of Chile: The 1997–1998 Dinámica del Clima de la Región de Antofagasta (DICLIMA) experiment. Journal of Geophysical Research 108 (D17), 4538.
Sarnthein, M., Tetzlaff, G., Koopmann, B., Wolter, K., Pflaumann, U., 1981. Glacial and interglacial wind regimes over the eastern subtropical Atlantic and north-west Africa. Nature 293 (5829), 193.
Scheidegger, K.F., Krissek, L.A., 1982. Dispersal and deposition of eolian and fluvial sediments off Peru and northern Chile. Geological Society of American Bulletin 93 (2), 150–162.
Schwerdtfeger, W., 1976. Climates of Central and South America. World Survey of Climatology, 12. Elsevier, Amsterdam.
Strub, P.T., Mesías, J.M., Montecino, V., Rutllant, J., Salina, S., 1998. Coastal ocean circulation off Western South America. In: Robinson, A.R., Brink, K.H. (Eds.), The Global Coastal Ocean. The Sea, vol. 11. John Wiley & Sons Inc., New York.
Stuut, J.-B.W., Prins, M.A., Schneider, R.R., Weltje, G.J., Jansen, J.H.F., Postma, G., 2002. A 300-kyr record of aridity and wind strength in southwestern Africa: inferences from grain-size distributions of sediments on Walvis Ridge, SE Atlantic. Marine Geology 180, 221–233.
Stuut, J.-B.W., Zabel, M., Ratmeyer, V., Helmke, P., 2005. Provenance of present-day eolian dust collected off NW Africa. Journal of Geophysical Research 110 (D04202), 1–14.
Stuut, J.-B., Marchant, M., Kaiser, J., Lamy, F., Mohtadi, M., Romero, O., Hebbeln, D., 2006. The late quaternary paleoenvironment of Chile as seen from marine archives. Geographica Helvetica 61 (2), 135–151.
Tanaka, T.Y., Chiba, M., 2006. A numerical study of the contributions of dust source regions to the global dust budget. Global and Planetary Change 52 (1–4), 88–104.
Tegen, I., et al., 2002. Impact of vegetation and preferential source areas on global dust aerosol: results from a model study. Journal of Geophysical Research 107 (D21), 4576.
Tucker, M.E., 1996. Methoden der Sedimentologie. Enke, Stuttgart.
Wagener, T., Guieu, C., Losno, R., Bonnet, S., Mahowald, N., 2008. Revisiting atmospheric dust export to the Southern Hemisphere ocean: biogeochemical implications. Global Biogeochemical Cycles 22 (GB2006), 1–13.
Weltje, G., 1997. End-member modeling of compositional data: Numerical-statistical algorithms for solving the explicit mixing problem. Mathematical Geology 29 (4), 503–549.
Weltje, G., Prins, M.A., 2003. Muddled or mixed? Inferring palaeoclimate from size distributions of deep-sea clastics. Sedimentary Geology 162, 39–62.
Werner, M., et al., 2002. Seasonal and interannual variability of the mineral dust cycle under present and glacial climate conditions. Journal of Geophysical Research 107 (D24), 4744.
Windom, H.L., 1976. Lithogenous material in marine sediments. In: Riley, J.P., Chester, R. (Eds.), Chemical Oceanography. Academic Press, London, pp. 103–135.
Wright, J.C.M., 2004. Evolution of the Galapagos Rise and the Bauer Microplate: Implications for the Nazca Plate. Texas A&M University, College Station.
Wyrtki, K., Meyers, G., 1976. The trade wind field over the Pacific ocean. Journal of Applied Meteorology 15 (7), 698–704.
Zeil, W., 1986. Südamerika. Geologie der Erde, 1. Enke, Stuttgart.